Supplementary Figures:

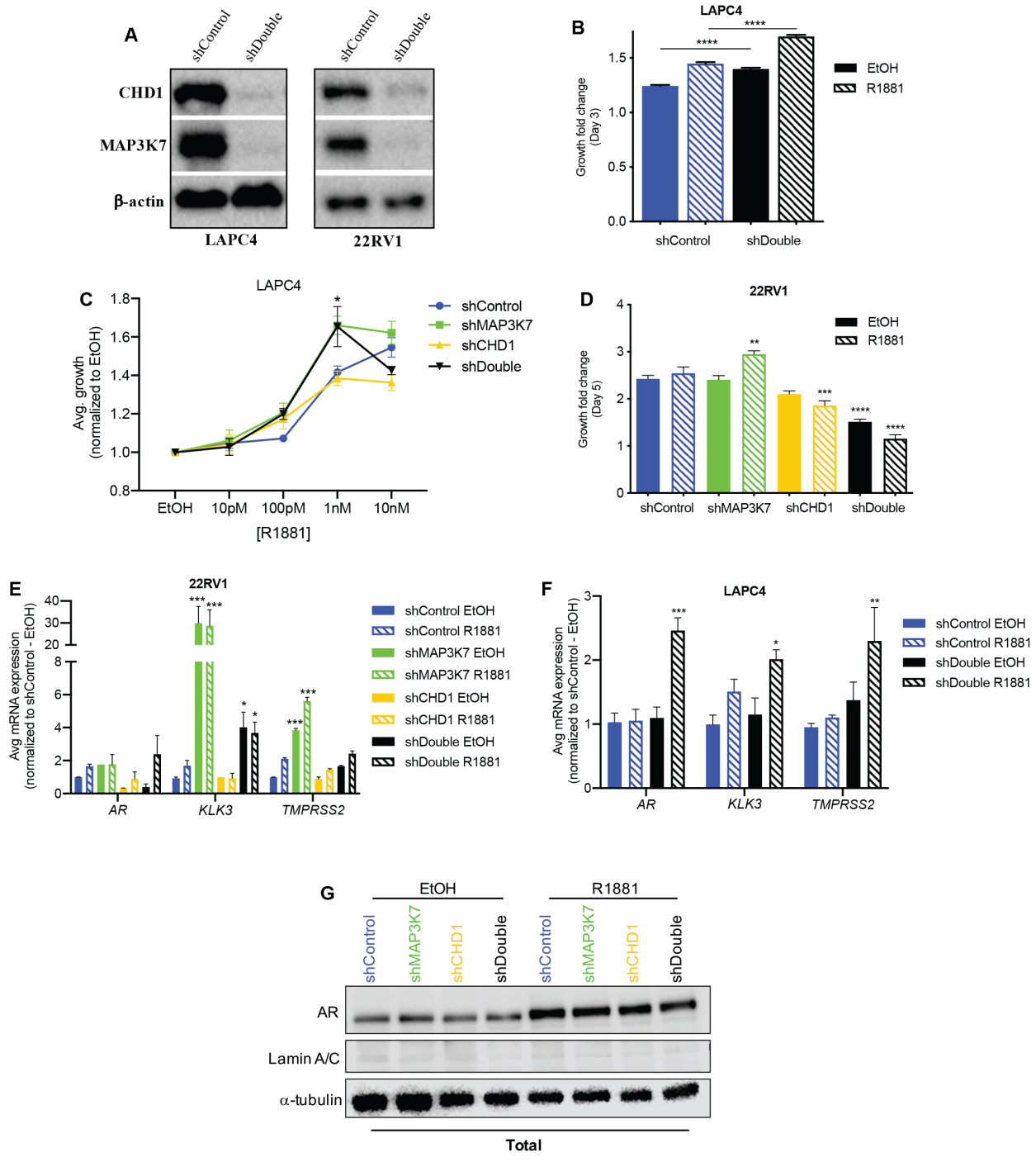

Supplemental Figure S1. Increased AR activity in other PCa cell lines with knockdown of *MAP3K7* and *CHD1*. (A) Western blot of shControl, shMAP3K7, shCHD1, and shMAP3K7-shCHD1 (shDouble) 22RV1 and LAPC4 cells. **(B)** Day 3 of growth assay for LAPC4 cells in

steroid-depleted medium ± 1 nM R1881 (n=3). **(C)** Day 5 of R1881 dose response curves for shControl, shMAP3K7, shCHD1, and shDouble LAPC4 cells normalized to EtOH treatment (n=3; p-values indicate comparison to shControl at respective doses). **(D)** Day 5 of growth assay for 22RV1 cells in steroid-depleted medium ± 1 nM R1881 (n=3; p-values indicate comparison to shControl EtOH). **(E)** RT-qPCR of *AR, KLK3* and *TMPRSS2* expression in 22RV1 or **(F)** LAPC4 cells cultured in steroid-depleted medium ± EtOH or 1 nM R1881 for 4 hr. Ct values normalized to *B2M* (22RV1) or *HPRT1* (LAPC4) expression and then to shControl (n=3; p-values represent comparison to shControl EtOH). **(G)** Representative western blot of AR protein in total fractions isolated from LNCaP cell lysates after treatment with ± 1 nM R1881 for 4 hr. Samples are from the same experiment as nuclear fractions in **Fig. 1G**. Data represent mean ± SEM; One-way ANOVA with Tukey's (B) or Dunnett's (D) multiple comparisons test, or two-way ANOVA with Dunnett's multiple comparisons test (C, E, F); *=$p<0.05$; **=$p<0.01$; ***=$p<0.001$; ****=$p<0.0001$.

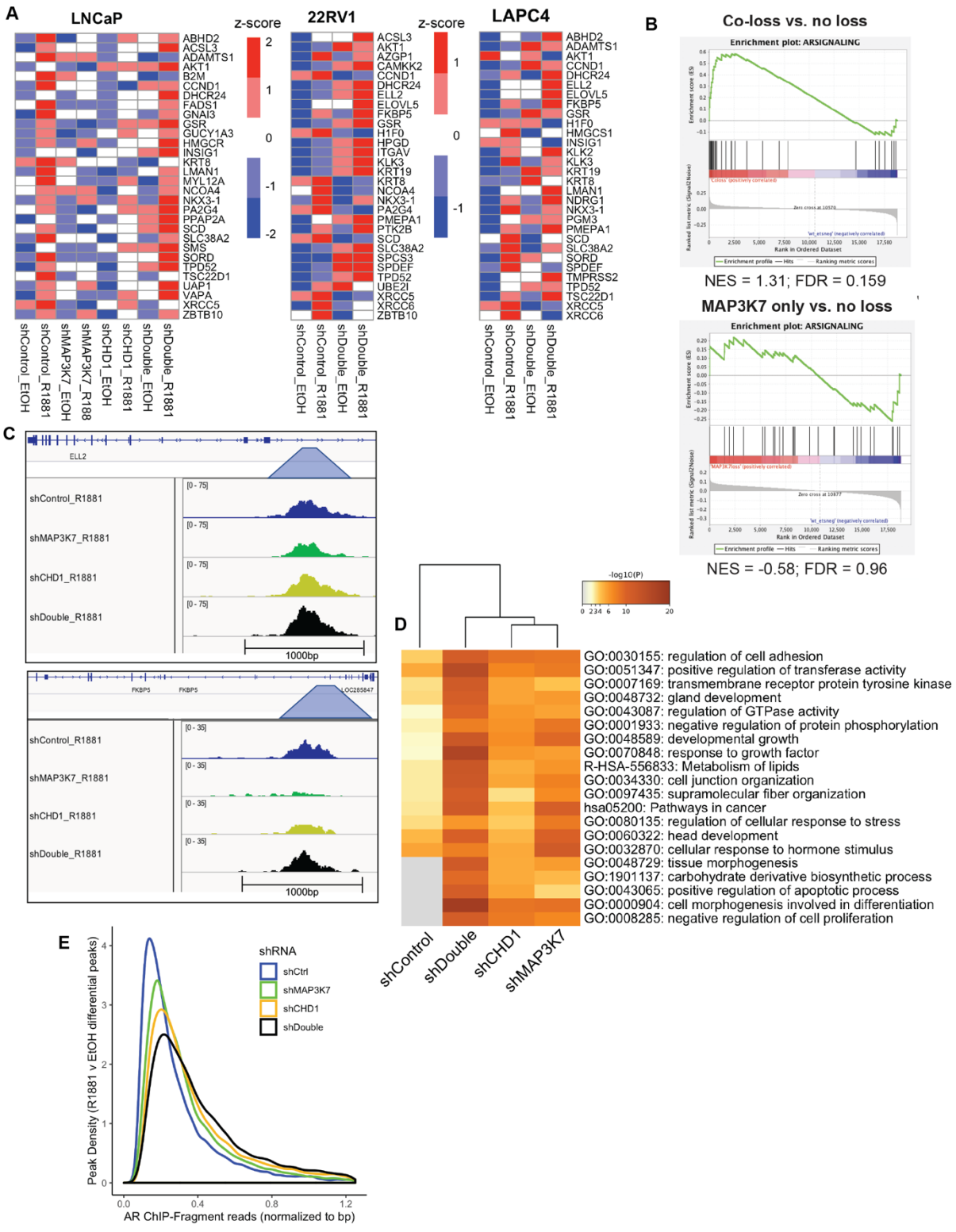

Supplemental Figure S2. Suppression of *MAP3K7* and *CHD1* increases AR signature gene expression and androgen-induced AR chromatin binding. (A) Heatmap illustration of z-score

expression changes of top 30 up-regulated AR signature genes (from MSigDB: M5908) in indicated cell types ± 1 nM R1881 for 4 hr. **(B)** GSEA of AR signaling gene signature in indicated MSKCC patient groups with copy number loss of *MAP3K7* or *MAP3K7* and *CHD1* versus patients with loss of neither. **(C)** IGV genome track images of AR ChIP-seq peaks at the *ELL2* (top) and *FKBP5* (bottom) loci. **(D)** Metascape pathway analysis of AR ChIP annotations with significant gene expression changes from Figure 2F-G. **(E)** Density plot of differential AR ChIP peaks (androgen-induced) between shControl, shMAP3K7, shCHD1, and shDouble R1881-treated versus respective EtOH-treated LNCaP cells (fold-change >4, Poisson p-value <1.00e-04).

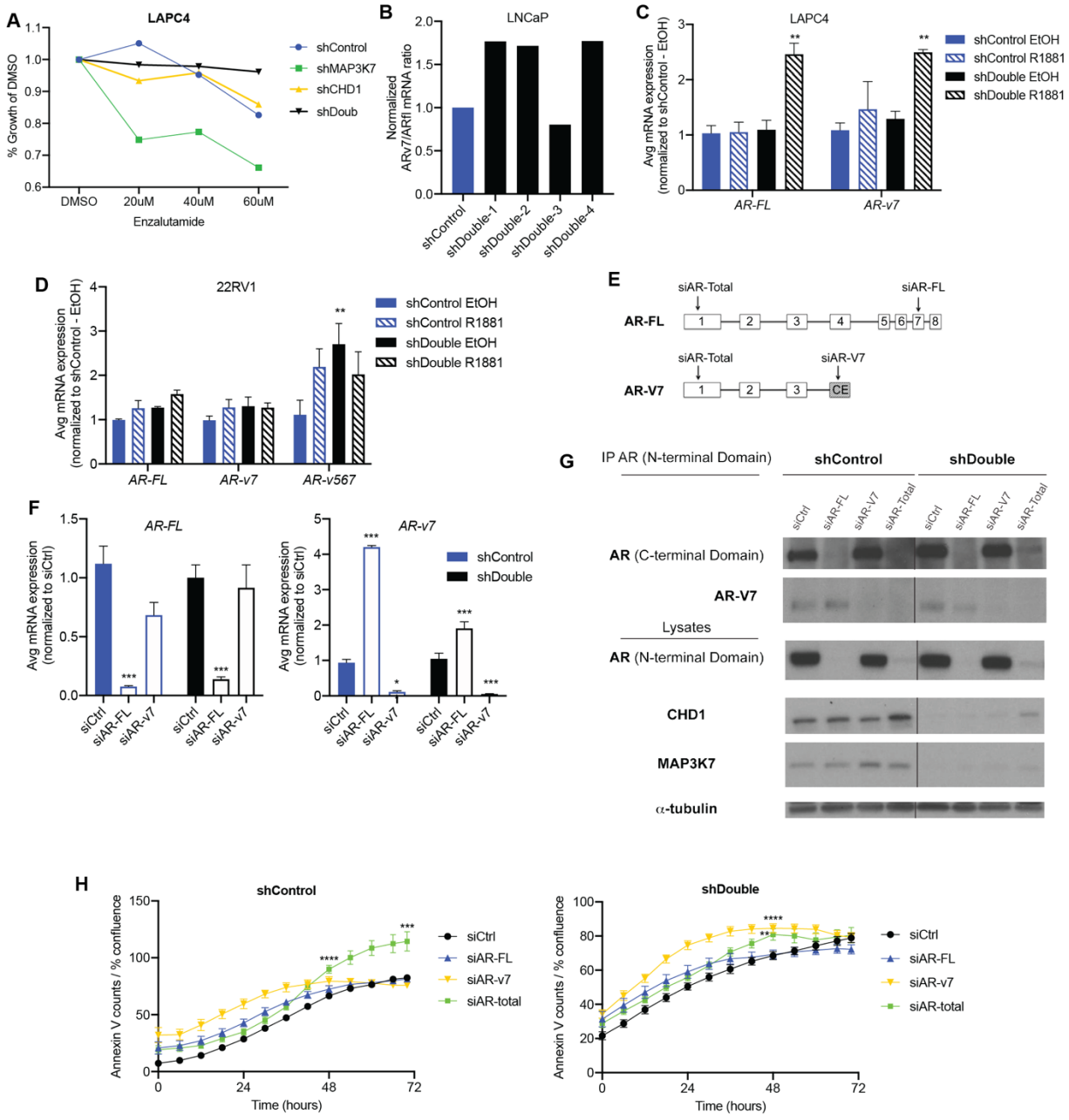

Supplemental Figure S3. AR variant expression in LAPC4 and 22RV1 cells. (A) Day 5 of growth assay for shControl and shDouble LAPC4 cells treated with 20-60 μM enzalutamide in castration conditions, normalized to DMSO treatment (n=3). **(B)** RT-qPCR of *AR-FL* and *AR-v7* showing an *AR-v7/AR-FL* ratio in multiple shDouble shRNA combinations compared to shControl LNCaP cells. Ct values normalized to *B2M* expression. **(C)** RT-qPCR of full-length

AR (*AR-FL*) and *AR-v7* gene expression in indicated LAPC4 cells ± 1 nM R1881 for 4 h. Ct values normalized to *HPRT1* expression and then to shControl (n=3; p-values represent comparison to shControl EtOH). **(D)** RT-qPCR of full-length AR (*AR-FL*), *AR-v7*, and *AR-v567* gene expression in indicated 22RV1 cells ± 1 nM R1881 for 4 h. Ct values normalized to *B2M* expression and then to shControl (n=3; p-values represent comparison to shControl EtOH). **(E)** Schematic of siRNA targeting constructs against AR-full length, AR-v7, and total AR. **(F)** RT-qPCR verification of siAR-FL and siAR-v7 targeting constructs in shControl and shDouble LNCaP cells 72 hours after transfection (n=3; p-values indicate comparison to siCtrl). **(G)** Immunoprecipitation western blot verification of siRNA targeting constructs in LNCaP cells. IP using AR N-terminal antibody, immunoblot with AR-C-terminal and AR-v7 antibodies. **(H)** Annexin V counts normalized to cell confluence of shControl (left) and shDouble (right) LNCaP cells in castration conditions beginning 24 hours after transfection with indicated siRNAs (n=3; p-values indicate comparison to siCtrl). Data represent mean ± SEM; two-way ANOVA with Dunnett's multiple comparisons test (C, D, F, H); *=$p<0.05$; **=$p<0.01$; ***=$p<0.001$; ****=$p<0.0001$.

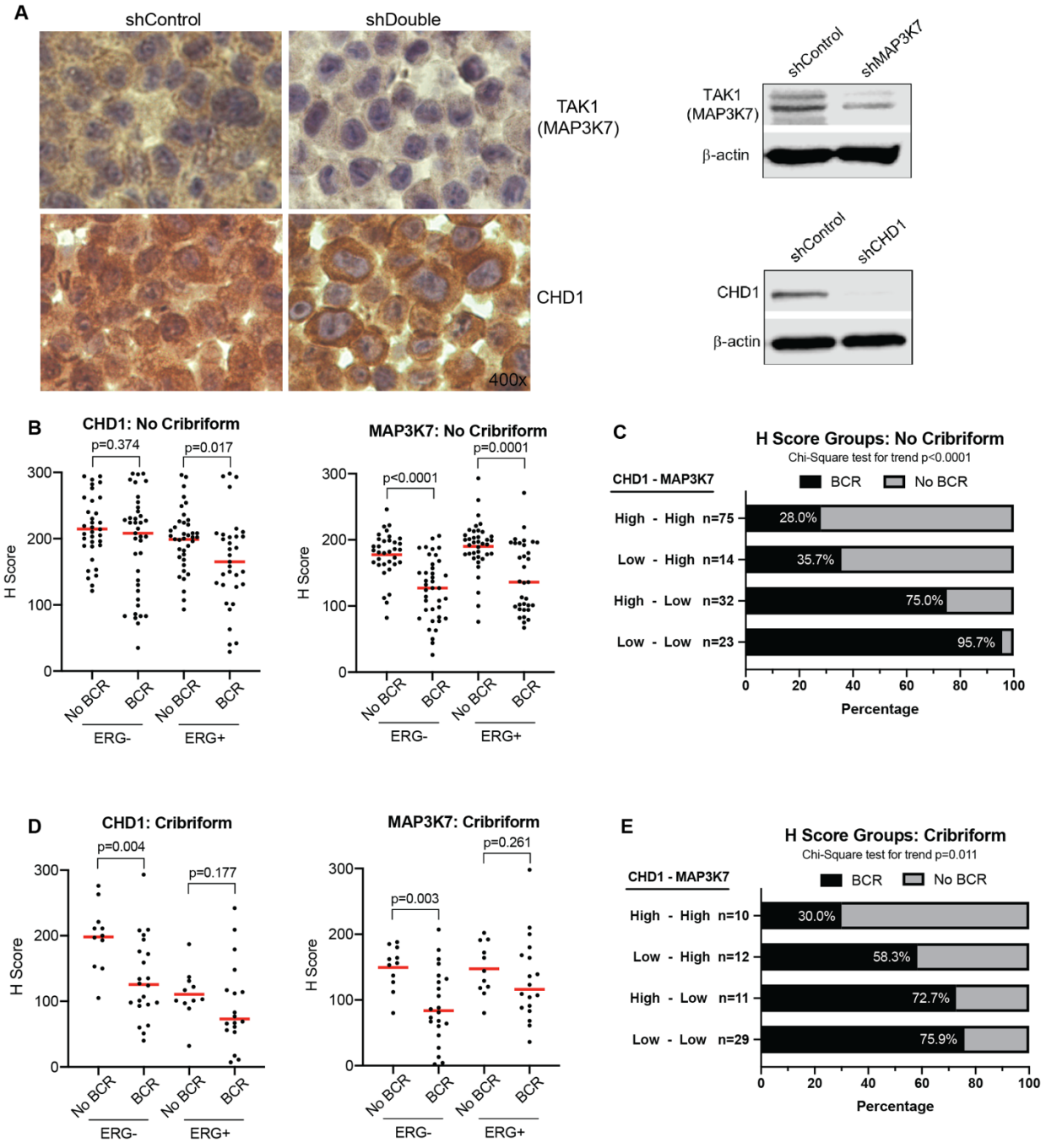

Supplemental Figure S4. MAP3K7 and CHD1 IHC expression in cribriform PCa.

(A) Verification of antibodies in indicated LNCaP cells via immunocytochemistry (left) and western blotting (right). **(B)** CHD1 and MAP3K7 immunohistochemical H-scores for 152 cases with no cribriform patterning. Cases are stratified by nuclear ERG positivity and then by

biochemical recurrence (BCR) or no BCR. **(C)** Frequency of BCR in non-cribriform cases with indicated combinations of high (>150) and low (<150) H-scores for MAP3K7 and CHD1. **(D)** CHD1 and MAP3K7 immunohistochemical H-scores for 62 cases with cribriform patterning. Cases are stratified by nuclear ERG positivity and then by biochemical recurrence (BCR) or no BCR. **(E)** Frequency of BCR in cribriform cases with indicated combinations of high (>150) and low (<150) H-scores for MAP3K7 and CHD1. Red bars (B, D) denote means. Wilcoxon rank sum test (B, D), Chi-Square test for trend (C, E).

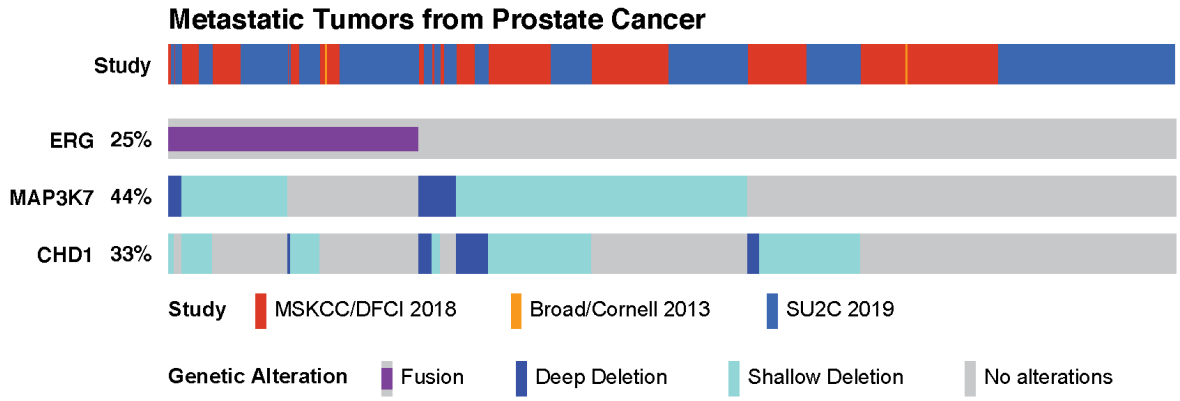

Supplemental Figure S5. Patient genomics meta-analysis of *MAP3K7* and *CHD1* deletions in metastatic PCa. Meta-analysis of multiple PCa genomic databases displaying frequency of *ERG* fusions and deletions of *MAP3K7* and *CHD1* in 753 metastatic PCa cases.

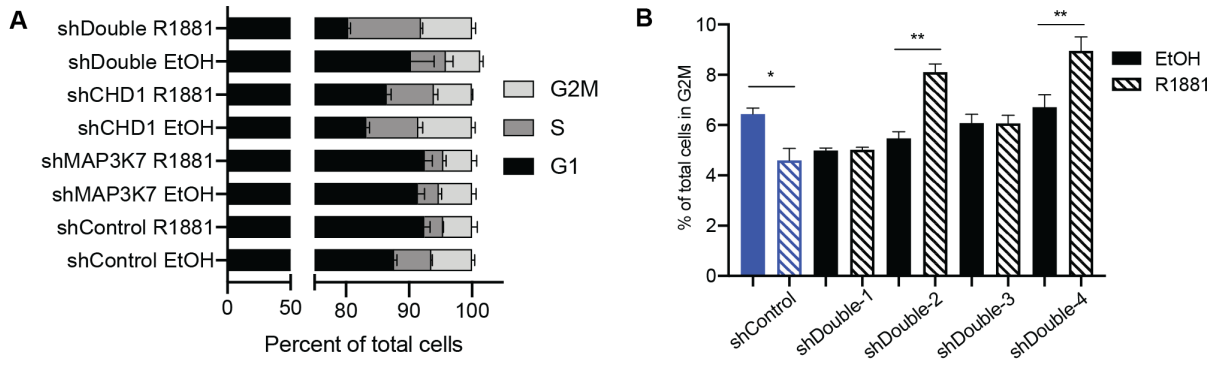

Supplemental Figure S6. Suppression of *MAP3K7* and *CHD1* alters progression through the cell cycle. (A) Flow cytometry cell cycle analysis of indicated LNCaP cells after 48 hours in steroid-depleted medium ± 1 nM R1881 showing percent of total cells in each cell stage (G1, S, G2M) (n=3). **(B)** Percent of cells in G2M cell stage for multiple shDouble shRNA construct combination (n=3). Data represent mean ± SEM; One-way ANOVA with Tukey's multiple comparisons test (B); *=$p<0.05$; **=$p<0.01$.